Fluorescence Turn-off-on probe based on polypyrrole/graphene quantum composites for selective and sensitive detection of paracetamol and ascorbic acid

Xiaotong Liu, Weidan Na, Hua Liu, Xingguang Su

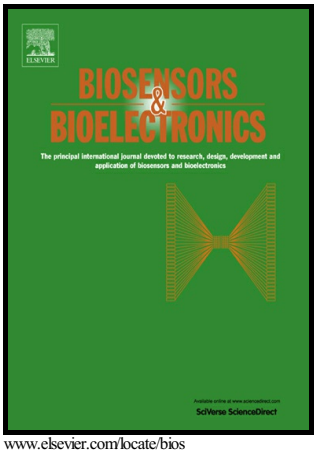

www.elsevier.com/locate/bios

PII: S0956-5663(17)30419-0
DOI: http://dx.doi.org/10.1016/j.bios.2017.06.044
Reference: BIOS9814

To appear in: *Biosensors and Bioelectronic*

Received date: 7 April 2017
Revised date: 14 June 2017
Accepted date: 21 June 2017

Cite this article as: Xiaotong Liu, Weidan Na, Hua Liu and Xingguang Su Fluorescence Turn-off-on probe based on polypyrrole/graphene quantun composites for selective and sensitive detection of paracetamol and ascorbic acic *Biosensors and Bioelectronic,* http://dx.doi.org/10.1016/j.bios.2017.06.044

Fluorescence Turn-off-on probe based on polypyrrole/graphene quantum composites for selective and sensitive detection of paracetamol and ascorbic acid

Xiaotong Liu, Weidan Na, Hua Liu, Xingguang Su*

Department of Analytical Chemistry, College of Chemistry, Jilin University, Changchun, 130012, China

*Corresponding author. Tel.: +86-0431-85168352. suxg@jlu.edu.cn

Abstract

In this work, we presented a novel biosensor for rapid detection of paracetamol and ascorbic acid. The novel biosensor was based on the fluorescent "turn off-on" of polypyrrole/graphene quantum dots (PPy/GQDs) composites. The composites exhibit strong fluorescence emission, which is dramatically enhanced as high as three times than that of pure GQDs. It is found that the fluorescence intensity of PPy/GQDs can be efficiently quenched by N-acetyl-p-benzoquinone (4-AOBQ), the oxidation product of paracetamol (PAR). And a turn-on fluorescence signal was observed when 4-AOBQ is reduced by ascorbic acid (AA). The quenched and recovered fluorescence intensity of PPy-GQDs was proportional to the concentration of PAR (0.067-233 μg/L) and AA (3.33-997.5 μg/L) respectively. The limit of detection is 0.022 μg/L for PAR and 1.05 μg/L for AA. The present method was applied to the determination of PAR and AA in human serum samples with satisfactory results.

Keywords: graphene quantum dots; polypyrrole; fluorescence; paracetamol; ascorbic acid

1 Introduction

As an effective and save analgesic agent, paracetamol (PAR, *N*-acetyl-p-aminophenol) is used worldwide for the relief of pain associated with neuralgia, cancer pain, arthralgia, cephalagra, headache, backache and postoperative pain (Yin et al. 2011). Paracetamol was firstly introduced into medicine as an antipyretic/analgesic by Von Mering in 1893 and has been in use as an analgesic for home medication for over 30 years. It is the most used medicine after acetylsalicylic acid in many countries as an alternative to aspirin and phenacetin (Bosch et al. 2006). However, large doses and chronic use of PAR or concomitant use with other drugs or alcohol can cause liver disorders, skin rashes, nephrotoxicity and inflammation of the pancreas (Prabakar and Narayanan 2007). It is also suggested that there is a possible association between the use of PAR during pregnancy and an increasing appearance of asthma in children (Li et al. 2014).

Ascorbic acid (AA), also known as Vitamin C, is an important vitamin known for its reductive properties, and is widely used as an antioxidant in food, beverages, animal feed, pharmaceutical formulations and so on (Kumar et al. 2008). AA has been an object of increasing interest in the pharmaceutical industry as it is a key component of anti-aging cosmetics for protecting the skin against UV-radiation and for stimulating collagen synthesis (Dumas et al. 1996).

Because of the importance role of PAR and AA play in biomedical fields, many analytical methods have been developed, including spectrophotometry (Mohamed et al. 1997), liquid chromatography (Shervington and Sakhnini 2000), capillary electrophoresis (Sultan et al. 2012), and electrochemical techniques (Bui et al. 2012; Hou et al. 2011). However, some of these

methods involve complicated pretreatment and complex instruments, and many of them are also have the disadvantages of time-consuming, expensive, laborious and unsuitable for rapid determination. Therefore, further development of high sensitivity and selectivity method for PAR and AA is desired.

Graphene quantum dots (GQDs), which combine the excellent properties of graphene and quantum dots, have attracted considerable attention in the fields of chemistry and biology. GQDs are a single layer or few-layer of carbon atoms in a closely packed honeycomb structure (Jiang et al. 2013). Compared with the conventional fluorescent probes (semiconductor quantum dots and organic fluorophores), GQDs simultaneously possess several key merits desirable for bioimaging and optical biosensing, including chemical inertness, high biocompatibility, stable photoluminescence, high electrical conductivity and good water-solubility (Dong et al. 2013; Kim et al. 2012). In recent years, polypyrrole (PPy) has become a booming and increscent investigated class of conjugated materials due to its excellent electronic, optical and thermal properties (Jeon et al. 2011). Based on these advantages, PPy has been found promising application in many different fields including supercapacitors, functional electrodes and sensors (Chatterjee et al. 2013; Yang et al. 2012).

In this study, we developed a facile fabrication of PPy/GQDs composites by synthesizing GQDs in the presence of PPy microspheres. The existence of amine groups on the PPy backbone may result in the fluorescent enhancement of GQDs by surface passivation (Dong et al. 2012; Shen et al. 2012). PPy/GQDs was used as simple, high selective and sensitive fluorescence probes for PAR and AA detection. As shown in Scheme.1, the phenolic hydroxyl group of the PAR could be oxidized to quinone by catalysis of tyrosinase (Tyr) (Yarman and Scheller 2016), and PAR is

converted to N-acetyl-p-benzoquinone (4-AOBQ). Thus, the fluorescence of PPy/GQDs could be efficiently quenched via an electron transfer process between PPy/GQDs and the quinone structure in 4-AOBQ. AA can reduce 4-AOBQ to 4-AOP (4-acetyla ainopyrocatechol), which does not have quinone structure, following the recovery of fluorescence of PPy/GQDs. The change of the fluorescence intensity of PPy/GQDs is proportional to the concentration of PAR and AA. Thus a fluorescence turn-off-on method for the sensing of two substances above was established. This system is very convenient, simple, rapid, and avoids the complex process of the GQDs' modification or immobilization.

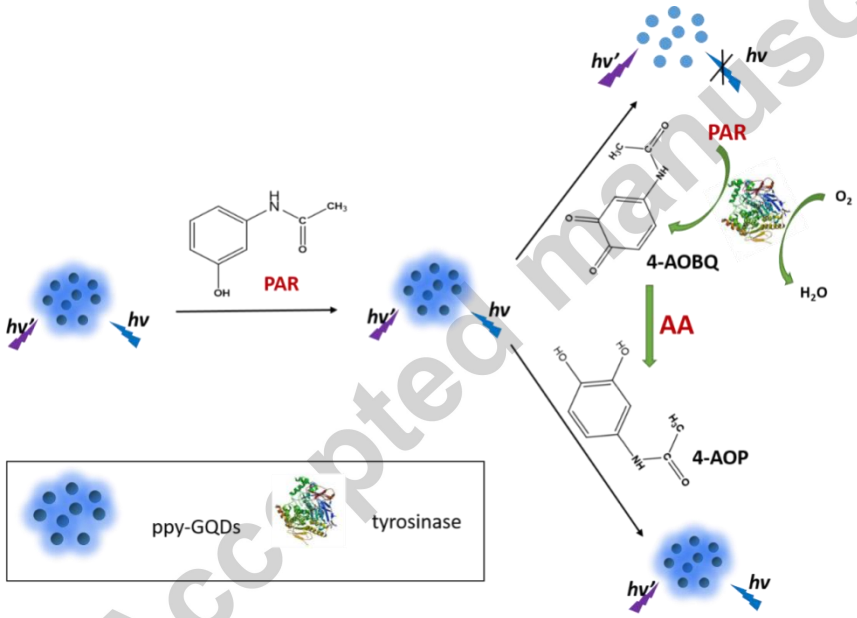

Scheme.1 Schematic illustration of the PPy/GQDs sensing system for the detection of PAR and AA.

2 Experiment

2.1 Reagents and chemicals

All chemicals used were at least of analytical reagent grade and used without further

purification. Hydrogen peroxide, NaOH, $FeCl_2$, Citric acid, Ascorbic acid, proline, tyrosine and glutamic acid were obtained from Beijing Dingguo Biotechnology Co. Ltd.Tyrosinase (500 U/mg), sodium dehydrogenized phosphate (NaH_2PO_4), disodium hydrogen phosphate (Na_2HPO_4) and sodium phosphate (Na_3PO_4) were purchased from Beijing Chemical Works. Alanine, serine, threonine, aspartic acid, glycine, lysine, were obtained from Sigma-Aldrich Chemical Co. Paracetamol tablets were obtained from Beijing Shuguang Pharmaceutical Co., Ltd. Ascorbic acid tablets were obtained from BY-HEALTH co. ltd. The water used in all experiments had a resistivity higher than 18 MΩ/ cm. The 10 mmol/L PBS buffered solution (pH=7.0) was used as the medium for detection process.

2.2 Instruments

The fluorescence spectra were obtained by using a Shimadzu RF-5301 PC spectrofluorophotometer equipped with a xenon lamp using right-angle geometry. UV-vis absorption spectra were obtained by a Varian GBC Cintra 10 e UV-vis spectrometer. In both experiments, a 1 cm path-length quartz cuvette was used. FT-IR spectra were recorded by a Bruker IFS66V FT-IR spectrometerequipped with a DGTS detector. All pH measurements were made with a PHS-3C pH meter (Tuopu Co., Hangzhou, China).

2.3 Synthesis of PPy microspheres

The PPy microspheres were prepared according to a typical preparation procedure (Zhou et al. 2015). Briefly, 5 mL H_2O_2 was added to the pyrrole/$FeCl_2$/H_2O (1 mL/0.1 g/94 mL) mixture and lasted for 6 h. After that, centrifugation was used for concentrating the products, and then washed several times with water to remove byproducts and unreacted reactants. The as prepared PPy

microspheres were dispersed in water at a concentration of 0.09 g PPy/40.00 g H_2O.

2.4 Synthesis of PPy/GQDs core/shell composites and GQDs

2 g citric acid (CA) monohydrate was heated to 200 °C in a 5 mL beaker by an oven, until the solid CA changed to a pale yellow liquid. Then, the liquid was added into 100 mL NaOH (10 mg/mL) solution in the presence of 200 μL of PPy dispersion. Preparation method of GQDs were as same as the approach mentioned above, but without the addition of PPy dispersion. The obtained PPy/GQDs solution was further dialyzed in a dialysis bag (retained molecular weight: 3500 Da) for 48 h to obtain GQDs. The solution was diluted five times for future use.

2.5 PAR detection

For PAR detection, different amount of PAR were added in a series of 1.5 mL solution containing 200 μL PPy/GQDs, 50 μL PBS (0.2 mol/L, pH=6.99) and 40 U/mL Tyr. Then the solution was incubated at 37 ℃ for 50 min. The fluorescence spectra were recorded between 400-670 nm wavelength range at the excitation wavelength of 370 nm. The slit width of emission and excitation were set at 5 nm and 10 nm respectively.

2.6 AA detection

For AA detection, different amount of AA were added in a series of 1.5 mL solution containing 200 μL PPy/GQDs, 50 μL PBS (0.2 mol/L, pH=6.99), 40 U/mL Tyr and 233 μg/L PAR. Then the solution was incubated at 25℃ for 45 min. The fluorescence spectra were recorded between 400-670 nm wavelength range at the excitation wavelength of 370 nm. The slit width of emission and excitation were set at 5 nm and 10 nm respectively.

2.7 Real sample assay

The blood samples of healthy persons were supplied by the Hospital of Changchun China, Japan Union Hospital. Some pretreatments to remove impurities are necessary before using in the experiment. First, acetonitrile is added to the blood samples (the volume of acetonitrile and blood was 1.5: 1) in 5 mL centrifuge tube. And then after shaking for 2 min at room temperature, the product was centrifuged at 10000 rpm for 10 min to remove protein. The supernatant was stored in −20 ℃ for future experiments. The obtained human serum samples were subjected to a 5-fold dilution, then a series of different concentrations of PAR and AA were added to prepare spiked samples which were detected by the method described above. All experiments were performed in compliance with the relevant laws and institutional guidelines, and the writing of informed consent for all samples was obtained from human subjects.

3 Results and discussion

3.1 Characterization and feasibility

The PPy/GQDs and GQDs were synthesized according to the method described above. The transmission Electron Microscopy (TEM) image of PPy/GQDs was showed in Fig. S1, which revealed that the PPy/GQDs was nearly spherical in shape with a diameter of 3.27 nm and mostly uniform in size. The optical properties of composites were characterized by the fluorescence and UV–vis absorption spectroscopy, shown in Fig.1 (A). It could be seen that the fluorescence emission peak of PPy/GQDs was at 475 nm. The UV-vis absorption spectra of GQDs shown in Fig.1 (A) indicated strong absorbance at 252 nm and a weak shoulder peak at around 348 nm,

which maybe result from π-π^* transition of aromatic structures and n-π^* transition of C=O, respectively (Fang et al. 2012; Novoselov et al. 2004). Fig.1 (B) shows that the fluorescence intensity (FL) of PPy/GQDs is three times higher than that of the free GQDs, which is owing to the surface passivation of GQDs through an acid–base type interaction between nitrogen atom on PPy and the carboxylic groups on GQDs (Routh et al. 2013). In addition, the PPy microspheres also accumulates the incompletely carbonized citric acid at the periphery of the composites via π–π interaction, which contributes to the surface passivation of GQDs (Dong et al. 2012). In Fig.1 (C), the majority characteristic peaks of PPy/GQDs could be clearly found, including 3429.05 cm^{-1}, which is ascribed to the hydroxyl groups linked to the composites, 1586.83 cm^{-1} and 2950.26 cm^{-1} due to the –COOH and $–CH_2$ bonding vibration, 1387.20 cm^{-1} from C–N bonding vibration of PPy (Routh et al. 2013).

To verify the detection method, we conducted feasibility studies. It can be seen from Fig.1 (D) that there was no significant change of the fluorescence intensity of PPy/GQDs after mixing with PAR, Tyr, AA separately or mixing with Tyr and AA at the same time. However, there was an obvious decrease of the fluorescence intensity after adding Tyr and PAR to the PPy/GQDs solution, then the fluorescence intensity recovered with the addition of AA. It was consistent with the mechanism with the addition of AA. It was consistent with the mechanism illustrated in Scheme.1.

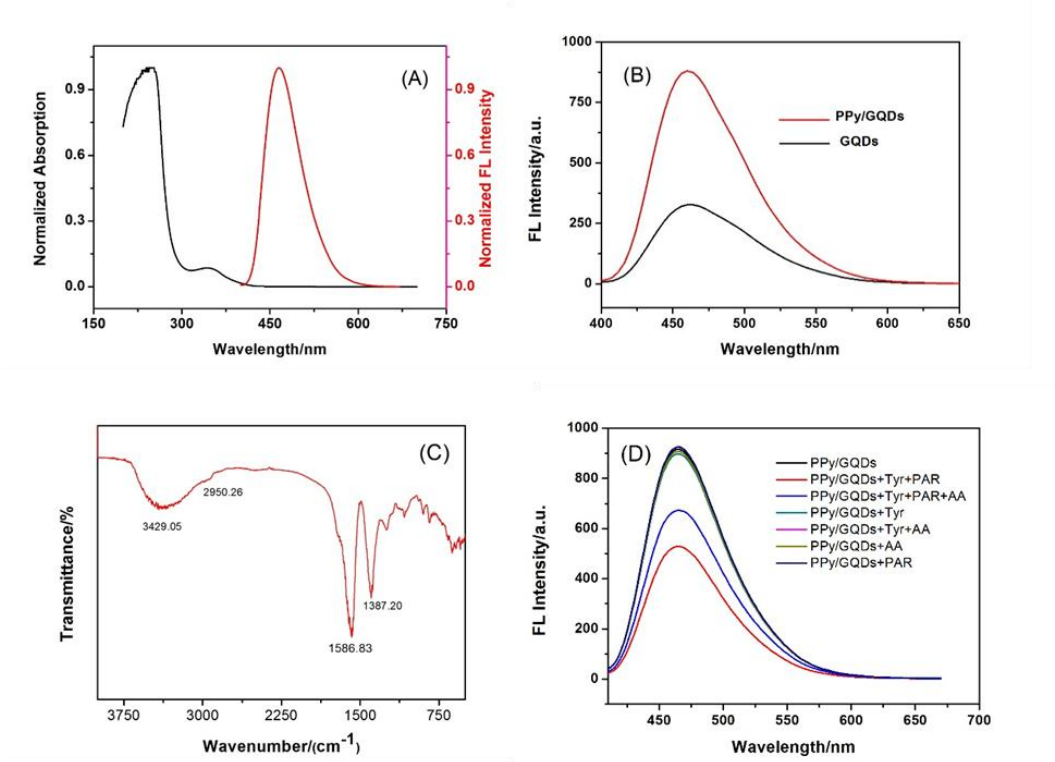

Fig.1 (A) The UV–vis absorption spectra, the fluorescence emission spectra of PPy/GQDs; (B) Fluorescence emission spectra of GQDs and PPy/GQDs; (C) The FTIR spectra of PPy/GQDs; (D) The fluorescence spectra of PPy/GQDs, PPy/GQDs+Tyr+PAR, PPy/GQDs+PAR+AA, PPy/GQDs+Tyr, PPy/GQDs+Tyr+AA, PPy/GQDs+AA, PPy/GQDs+PAR. Concentration: 200 μg/L PAR, 40 U/mL Tyr, 400 μg/L AA.

3.2 Optimization for PAR and AA detection

In order to optimize the conditions for PAR and AA detection, we studied the effects of incubation time, the concentration of Tyr, pH and temperature on the fluorescence intensity of PPy/GQDs. In this work, the reaction time was investigated firstly. The effect of incubating time on the detection of PAR with different concentrations of Tyr was shown in Fig.S2 (A). It can be observed that the fluorescence intensity of PPy/GQDs-Tyr-PAR system decreased rapidly in the first 20 min, then kept constant after 40 min. Thus the reaction time of 50 min was adopted in the detection of PAR for complete reaction. The effect of incubating time on the detection of AA was shown in Fig.S2 (B). It can be seen that the fluorescence intensity of PPy/GQDs-Tyr-PAR-AA

system increased rapidly in the first 25 min, then kept constant after 35 min. Thus the reaction time of 45 min was adopted in the detection of AA. Then we studied the effect of Tyr concentration on the assay of PAR. As illustrated in Fig.S2 (C), the fluorescence intensity decreased and got to a plateau when the concentration of Tyr was higher than 30 U/mL. In order to ensure the complete reaction, we set the concentration of Tyr at 40 U/mL. The effect of pH in the range of 5.52–7.58 on the fluorescence intensity of detection system was shown in Fig.S2 (D). It can be observed that the fluorescence intensity of the system approached to the maximum at pH 7.0 for both PAR and AA detection, relatively. So we chose PBS buffer solution (pH=7.0) in the future experiments. Then we optimize the reaction temperature. As shown in Fig.S2 (E) and Fig.S2 (F), the fluorescence intensity of the system reached highest at 37 ℃ for the detection of PAR and lowest at 25 ℃ for the detection of AA. Thus, the optimized temperature for the detection of PAR and AA is 37 ℃ and 25 ℃, respectively.

3.3 Detection of PAR

The quenching effect of PAR on the fluorescence intensity of PPy/GQDs-Tyr system was studied first. Fig.2 shows that in the presence of Tyr, the fluorescence intensity of PPy/GQDs-Tyr system gradually decreased with the increase of PAR concentration in the range of 0–666.7 μg/L. And the inset showed there was a good linear relationship between the relative fluorescence intensity I/I_0 (I and I_0 were the fluorescence emission intensity of the PPy/GQDs-Tyr system in the presence and absence of PAR, respectively.) and the concentration of PAR in the range of 0.067-233 μg/L, with a detection limit of 0.022 μg/L. The linear regression equation was

$$I/I_0 = 0.98524 - 0.00288 C_{PAR}\ (\mu g/L)$$

The corresponding regression coefficient (R^2) was 0.996. The detection limit was based on the equation LOD=3σ/s, where σ was the standard deviation of the blank signals of the PPy/GQDs-Tyr system and s was the slope of the calibration curve. 233 μg/L PAR was chosen for AA detection in the next experiment. The dynamic range of the fluorescence signal versus the concentration of PAR was shown in Fig.S3.

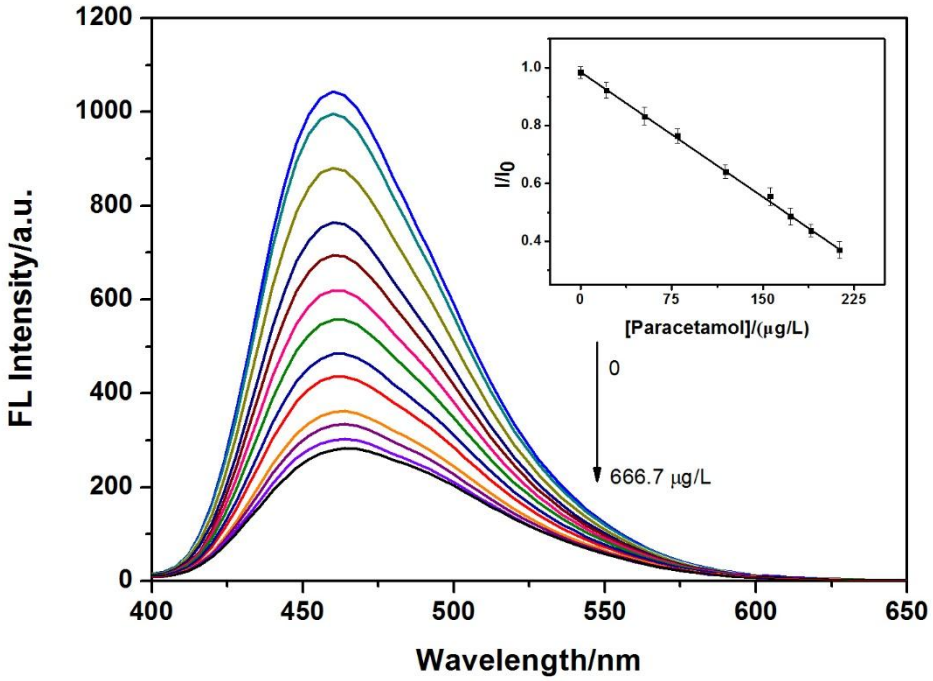

Fig.2 The fluorescence spectra of PPy/GQDs-Tyr system with different concentrations of PAR in the range of 0–666.7 μg/L (0, 33.3, 53.3, 66.7, 133.3, 166.7,180, 233.3, 266.7, 300, 466.7, 533.3, 666.7 μg/L). The inset showed the relationship between I/I_0 and the concentration of PAR in the range of 0.067-233 μg/L. I and I_0 were the fluorescence emission intensity of the detection system in the presence and absence of PAR, respectively. The error bars (RSD) were gained from three parallel test results.

3.4 Detection of AA

Under optimized conditions, the relationship between the fluorescence intensity of PPy/GQDs-Tyr-PAR-AA system and the concentration of AA was investigated. As shown in Fig.3, the fluorescence intensity of PPy/GQDs-Tyr-PAR-AA system was obviously restored with the

increase of AA concentration. Fig.3 inset showed there was a good linear relationship between the relative fluorescence intensity I/I_1 (I and I_1 were the fluorescence emission intensity of the PPy/GQDs-Tyr-PAR system in the presence and absence of AA, respectively) and the concentration of AA in the range of 3.33-997.5 μg/L. The linear regression equation was:

$$I/I_1=1.069+0.00265C_{AA}\,(\mu g/L)$$

The correlation coefficient R^2=0.997. And the detection limit for AA was1.05 μg/L. The dynamic range of the fluorescence signal versus the concentration of AA was shown in Fig.S4.

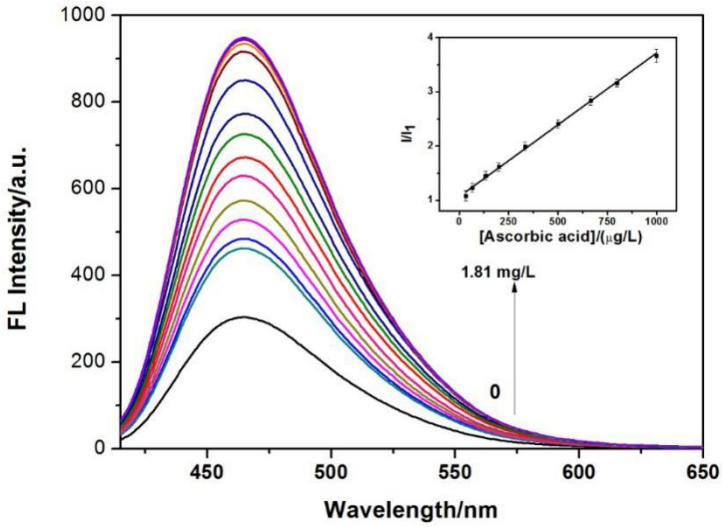

Fig.3 The fluorescence spectra of PPy/GQDs-Tyr-PAR system (CPAR=233 μg/L) with different concentrations of AA in the range of 0–1.81 mg/L（0, 0.033, 0.067, 0.12, 0.21, 0.33, 0.510, 0.67, 0.81, 0.99, 1.33, 1.57, 1.81 mg/L）. The inset showed the relationship between I/I_1 and the concentration of AA in the range of 3.33-997.5 μg/L. I and I_1 were the fluorescence emission intensity of the detection system in the presence and absence of AA, respectively. The error bars (RSD) were gained from three parallel test results.

A comparison of detection limits and linear ranges between this method and some other methods for PAR and AA determination reported previously was listed in Table.S1 and Table.S2. Compared with other methods, the method we established offered a comparable or superior linear range and detection limit.

3.5 Interference study

To further testify the selectivity of the present fluorescence method, we investigated the fluorescence response of the sensing system to other interfering substances included Na^+ (2000 μmol/L), K^+ (2000 μmol/L), Ca^{2+} (2000 μmol/L), alanine (Ala) (1000 μg/L), serine (Ser) (1000 μg/L), threonine (Thr) (1000 μg/L), glycin (Gly) (1000 μg/L), proline (Pro) (1000 μg/L), aspartic acid (Asp) (1000 μg/L) and lysine (Lys) (1000 μg/L). In Fig.4, blank represented the fluorescence intensity of the sensing system for PAR (100 μg/L) and AA (100 μg/L) detection without target analytes, respectively. The results indicated that common metal ions and biomolecules had no obvious interference on the detection for PAR and AA.

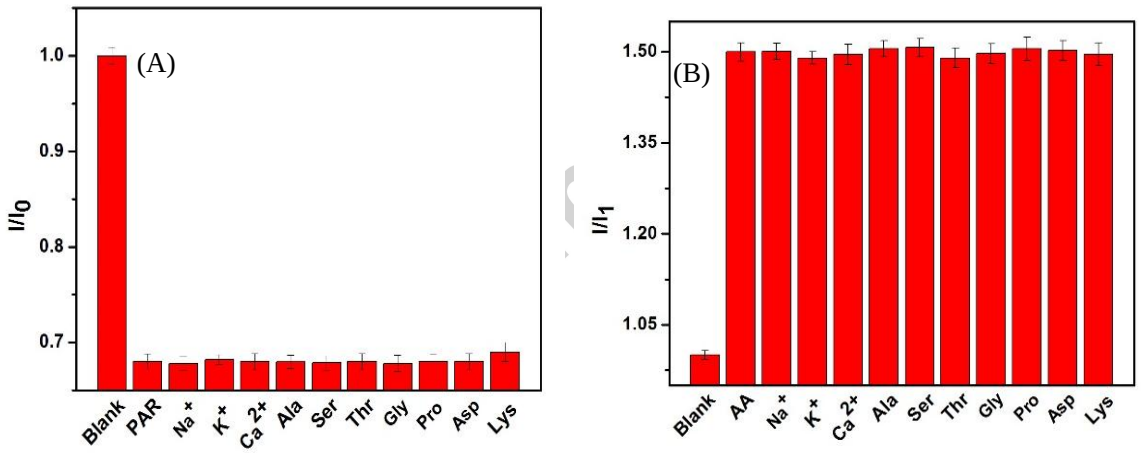

Fig.4 The interference of potentially interfering substances (Na^+ (2000 μmol/L), K^+ (2000 μmol/L), Ca^{2+} (2000 μmol/L), alanine (Ala) (1000 μg/L), serine (Ser) (1000 μg/L), threonine (Thr) (1000 μg/L), glycin (Gly(1000 μg/L)), proline (Pro) (1000 μg/L), aspartic acid (Asp) (1000 μg/L) and lysine (Lys) (1000 μg/L) on the determination sensing system for **(A)** PAR (100 μg/L) and **(B)** AA (100 μg/L) determination.

3.6 Real samples detection

In order to further demonstrate the practicality of the present fluorescence method, we used the fluorescence sensing system for the detected PAR and AA in human serum. The concentration

was determined by the standard addition method and the results were listed in Table.1. It was found that the recovery of PAR and AA is in the range of 97.5-102.7% and 99.3-102.3%, relatively. The relative standard deviation (RSD) was no more than 2.13%. These results demonstrated that the proposed method has potential application in practical measurement of PAR and AA.

Table.1 Determination of the PAR and AA in human serum samples

	Samples[a]	Added (μg/L)	Total found (μg/L)	Recovery (%)	RSD (%, n=3)
PAR	0	0	0.12	-	0.27
	1	0.3	0.41	98.4	1.56
	2	0.5	0.63	102.7	1.43
	3	1.0	1.0	97.5	0.96
AA	0	0	38.77	-	1.98
	1	30	68.95	100.6	2.13
	2	50	79.92	102.3	1.78
	3	80	108.12	99.3	2.09

[a] Human serum samples were 5-time diluted with deionized water.

4 Conclusion

In summary, we have developed a novel biosensor for rapid detection of paracetamol and ascorbic acid based on the fluorescent “turn off-on” of polypyrrole/graphene quantum dots (PPy/GQDs) composites. Under the optimized conditions, good linear relationships were obtained between the relative fluorescence intensity and the concentrations of PAR or AA in the range of

0.067-233 μg/L or 3.33-997.5 μg/L, respectively. Moreover, the proposed method was successfully applied to the detection of PAR and AA in human serum samples with good results. In comparison with the previous reports, the proposed method is simple, low cost, rapid, and avoids the complex process of the GQDs' modification or immobilization. We believe that the probe can be promoted for a lot of practical applications in chemical, environmental and biological systems.

Acknowledgements

This work was finally supported by the National Natural Science Foundation of China (No. 21075050 and No. 21275063), the Science and Technology Development project of Jilin province, China (No.20150204010GX).

References

Bosch, M.E., Sánchez, A.J.R., Rojas, F.S., Ojeda, C.B., 2006. Determination of paracetamol: Historical evolution. Journal of Pharmaceutical and Biomedical Analysis 42(3), 291-321.

Bui, M.-P.N., Li, C.A., Han, K.N., Pham, X.-H., Seong, G.H., 2012. Determination of acetaminophen by electrochemical co-deposition of glutamic acid and gold nanoparticles. Sensors and Actuators B: Chemical 174, 318-324.

Chatterjee, S., Shit, A., Nandi, A.K., 2013. Nanochannel morphology of polypyrrole-ZnO nanocomposites towards dye sensitized solar cell application. Journal of Materials Chemistry A 1(39), 12302-12309.

Dong, Y., Li, G., Zhou, N., Wang, R., Chi, Y., Chen, G., 2012. Graphene Quantum Dot as a Green and Facile Sensor for Free Chlorine in Drinking Water. Analytical Chemistry 84(19), 8378-8382.

Dong, Y., Pang, H., Yang, H.B., Guo, C., Shao, J., Chi, Y., Li, C.M., Yu, T., 2013. Carbon-Based Dots Co-doped with Nitrogen and Sulfur for High Quantum Yield and Excitation-Independent Emission. Angewandte Chemie-International Edition 52(30), 7800-7804.

Dumas, M., Chaudagne, C., Bonte, F., Meybeck, A., 1996. Age-related response of human dermal fibroblasts to L-ascorbic acid: study of type I and III collagen synthesis. Comptes rendus de l'Academie des sciences. Serie III, Sciences de la vie 319(12), 1127-1132.

Fang, Y., Guo, S., Li, D., Zhu, C., Ren, W., Dong, S., Wang, E., 2012. Easy Synthesis and Imaging Applications of Cross-Linked Green Fluorescent Hollow Carbon Nanoparticles. ACS Nano 6(1), 400-409.

Hou, X., Shen, G., Meng, L., Zhu, L., Guo, M., 2011. Multi-walled carbon nanotubes modified glass carbon electrode and its electrocatalytic activity towards oxidation of paracetamol. Russian Journal of Electrochemistry 47(11), 1262-1267.

Jeon, S.S., Kim, C., Ko, J., Im, S.S., 2011. Spherical polypyrrole nanoparticles as a highly efficient counter electrode for dye-sensitized solar cells. Journal of Materials Chemistry 21(22), 8146-8151.

Jiang, F., Chen, D., Li, R., Wang, Y., Zhang, G., Li, S., Zheng, J., Huang, N., Gu, Y., Wang, C., Shu, C., 2013. Eco-friendly synthesis of size-controllable amine-functionalized graphene quantum dots with antimycoplasma properties. Nanoscale 5(3), 1137-1142.

Kim, S., Hwang, S.W., Kim, M.-K., Shin, D.Y., Shin, D.H., Kim, C.O., Yang, S.B., Park, J.H., Hwang, E., Choi, S.-H., Ko, G., Sim, S., Sone, C., Choi, H.J., Bae, S., Hong, B.H., 2012. Anomalous Behaviors of Visible Luminescence from Graphene Quantum Dots: Interplay between Size and Shape. ACS Nano 6(9), 8203-8208.

Kumar, S.A., Lo, P.-H., Chen, S.-M., 2008. Electrochemical selective determination of ascorbic acid at redox active polymer modified electrode derived from direct blue 71. Biosensors and Bioelectronics 24(4), 518-523.

Li, J., Liu, J., Tan, G., Jiang, J., Peng, S., Deng, M., Qian, D., Feng, Y., Liu, Y., 2014. High-sensitivity paracetamol sensor based on Pd/graphene oxide nanocomposite as an enhanced electrochemical sensing platform. Biosensors and Bioelectronics 54, 468-475.

Mohamed, F.A., AbdAllah, M.A., Shammat, S.M., 1997. Selective spectrophotometric determination of p-aminophenol and acetaminophen. Talanta 44(1), 61-68.

Novoselov, K.S., Geim, A.K., Morozov, S.V., Jiang, D., Zhang, Y., Dubonos, S.V., Grigorieva, I.V., Firsov, A.A., 2004. Electric Field Effect in Atomically Thin Carbon Films. Science 306(5696), 666-669.

Prabakar, S.J.R., Narayanan, S.S., 2007. Amperometric determination of paracetomol by a surface modified cobalt hexacyanoferrate graphite wax composite electrode. Talanta 72(5), 1818-1827.

Routh, P., Das, S., Shit, A., Bairi, P., Das, P., Nandi, A.K., 2013. Graphene Quantum Dots from a Facile Sono-Fenton Reaction and Its Hybrid with a Polythiophene Graft Copolymer toward Photovoltaic Application. ACS Applied Materials & Interfaces 5(23), 12672-12680.

Shen, J., Zhu, Y., Yang, X., Li, C., 2012. Graphene quantum dots: emergent nanolights for bioimaging, sensors, catalysis and photovoltaic devices. Chemical Communications 48(31), 3686-3699.

Shervington, L.A., Sakhnini, N., 2000. A quantitative and qualitative high performance liquid chromatographic determination of acetaminophen and five of its para-substituted derivatives. Journal of Pharmaceutical and Biomedical Analysis 24(1), 43-49.

Sultan, M.A., Maher, H.M., Alzoman, N.Z., Alshehri, M.M., Rizk, M.S., Elshahed, M.S., Olah, I.V., 2012. Capillary Electrophoretic Determination of Antimigraine Formulations Containing Caffeine, Ergotamine, Paracetamol and Domperidone or Metoclopramide. Journal of Chromatographic Science 51(6), 502-510.

Yang, C., Xu, C., Wang, X., 2012. ZnO/Cu Nanocomposite: A Platform for Direct Electrochemistry of Enzymes and Biosensing Applications. Langmuir 28(9), 4580-4585.

Yarman, A., Scheller, F.W., 2016. MIP-esterase/Tyrosinase Combinations for Paracetamol and Phenacetin. Electroanalysis 28(9), 2222-2227.

Yin, H., Shang, K., Meng, X., Ai, S., 2011. Voltammetric sensing of paracetamol, dopamine and 4-aminophenol at a glassy carbon electrode coated with gold nanoparticles and an organophillic layered double hydroxide. Microchimica Acta 175(1), 39.

Zhou, X., Ma, P., Wang, A., Yu, C., Qian, T., Wu, S., Shen, J., 2015. Dopamine fluorescent sensors based on polypyrrole/graphene quantum dots core/shell hybrids. Biosensors and Bioelectronics 64, 404-410.

Highlights:

- PPy/GQDs with a fluorescence emission peak of 475 nm were used to detect paracetamol (PAR) and ascorbic acid (AA).
- The fluorescence intensity of PPy/GQDs was as high as three times than that of pure GQDs.
- The detection of PAR and AA was based on turn-off-on fluorescent strategy.
- The proposed method was simple, low cost and had a higher sensitivity and better selectivity.
- The proposed method was applied to the determination of PAR and AA in human serum samples with satisfactory results.